# Design, alignment, and deployment of the Hobby Eberly Telescope prime focus instrument package

Vattiat, Brian, Hill, Gary, Lee, Hanshin, Moreira, Walter, Drory, Niv, et al.

Brian Vattiat, Gary J. Hill, Hanshin Lee, Walter Moreira, Niv Drory, Jason Ramsey, Linda Elliot, Martin Landriau, Dave M. Perry, Richard Savage, Herman Kriel, Marco Häuser, Florian Mangold, "Design, alignment, and deployment of the Hobby Eberly Telescope prime focus instrument package," Proc. SPIE 9147, Ground-based and Airborne Instrumentation for Astronomy V, 91474J (24 July 2014); doi: 10.1117/12.2056407

SPIE.

Event: SPIE Astronomical Telescopes + Instrumentation, 2014, Montréal, Quebec, Canada

# Design, alignment, and deployment of the Hobby Eberly Telescope prime focus instrument package

Brian Vattiat[a], Gary J. Hill[a], Hanshin Lee[a], Walter Moreira[a], Niv Drory, Jason Ramsey[a], Linda Elliot[a], Martin Landriau[a], Dave M Perry[a], Richard Savage[a], Herman Kriel[a], Marco Haeuser[b], Florian Mangold[b]

[a]McDonald Observatory, Univ. of Texas at Austin, 1 University Station C1402, Austin, TX 78712, USA; [b]Ludwig Maximilian University of Munich, Geschwister-Scholl-Platz 1, 80539 Munich, Germany

## ABSTRACT

The Hobby-Eberly Telescope (HET) is undergoing an upgrade to increase the field of view to 22 arc-minutes with the dark energy survey HETDEX the initial science goal [1]. Here we report on the design, alignment, and deployment of a suite of instruments located at prime focus of the upgraded HET. This paper reviews the integration of motion control electronics and software and alignment of those electromechanical systems. Use of laser trackers, alignment telescopes, and other optical alignment techniques are covered. Deployment onto the upgraded telescope is discussed.
**Keywords:** HETDEX, HET, Hobby Eberly Telescope, VIRUS

## 1. INTRODUCTION

The Hobby Eberly Telescope (HET) is a unique telescope built in far west Texas. The telescope primary mirror consists of 91 individual spherical segments mounted on a structure with fixed altitude and moveable azimuth. The Prime Focus Instrument Package is mounted to a 6 degree-of-freedom stage [2],[3] above the primary mirror, allowing the telescopes field of view to track celestial objects. Figure 1 shows renderings of the upgraded telescope and the Prime Focus Instrument Package (PFIP). Problems with the Wide Field Corrector (WFC) during final assembly at the University of Arizona's College of Optical Sciences have forced a delay in the deployment of PFIP and therefore are not covered in this paper as expected.

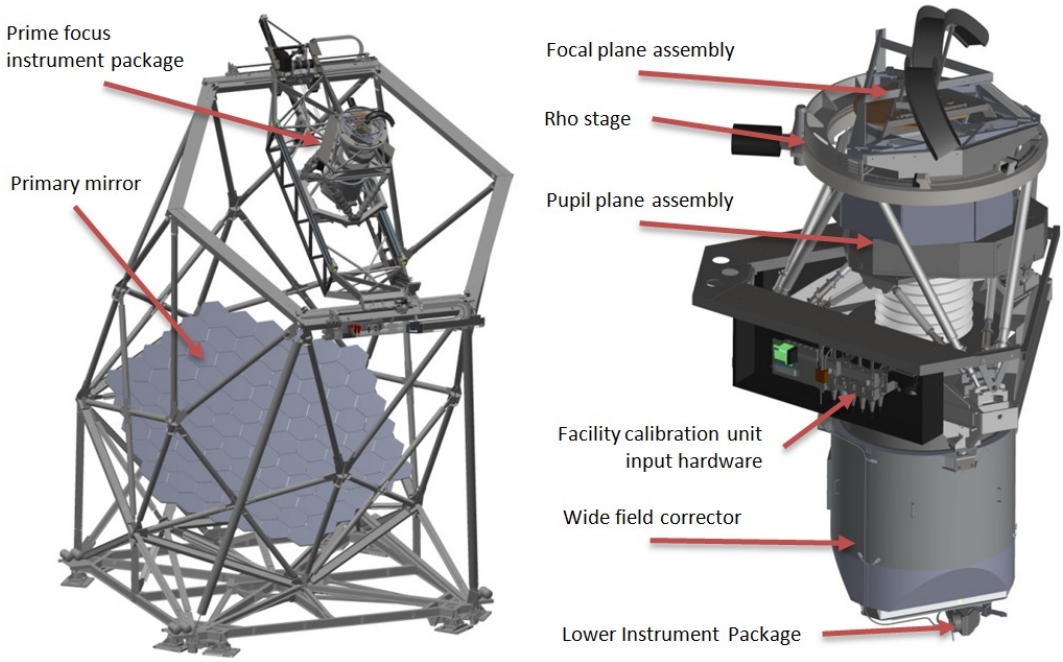


Figure 1. Renderings of the HET telescope and the prime focus instrument package

Ground-based and Airborne Instrumentation for Astronomy V, edited by Suzanne K. Ramsay, Ian S. McLean, Hideki Takami, Proc. of SPIE Vol. 9147, 91474J · © 2014 SPIE · CCC code: 0277-786X/14/$18 · doi: 10.1117/12.2056407

# 2. CONTROL SYSTEM

## 2.1 Instrument control

The instrumentation contained in PFIP includes guide probes, wave front sensors, acquisition camera, deployable fold mirrors, filter wheels, and a shutter. The electromechanical designs of these subsystems have been previously discussed in detail [4],[5]. In all, PFIP consists of 13 servo actuators, 8 pneumatic actuators, 8 power relays, and various hall-effect position and limit sensors. All actuators and sensors interface to a National Instruments CompactRIO embedded controller which is mounted in the Focal Plane Assembly utilities enclosure. The controller is a model NI-9022 mated to a model NI-9112 chassis with 8 module slots and a Virtex-5 LX 30 FPGA. The servo motor controllers, all Maxon EPOS2 positioning controllers, interface with the CompactRIO controller via a NI-9862 CAN interface module. The pneumatic actuators and power relays interface to sourcing outputs of two NI-9472 digital output modules. Hall effect position sensors are connected to either the servo controllers directly or sinking inputs of a NI-9421 digital input module. An Ethernet connection is used to interface the CompactRIO controller to the broader Telescope Control System (TCS), with EPICS being used to provide cross-platform communication. Figure 2, below illustrates the control system connectivity.

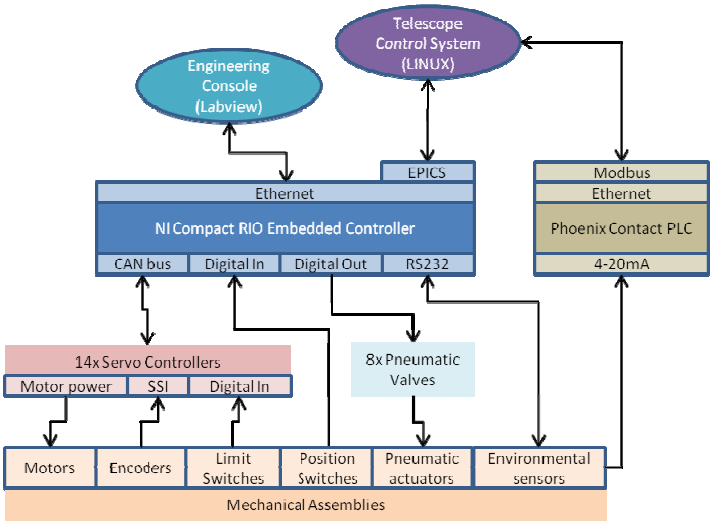


Figure 2. Control system schematic of PFIP

The CompactRIO controller is programmed using the National Instruments LabView software environment. Two layers of programming are used for the controller; the real-time operating system and the underlying FPGA. The FPGA layer handles the signal-level communications between the real-time operating system and the hardware. CAN-specific software is required at the FPGA layer to handle the high speed digital IO. Maxon provides a free software library for the CompactRIO FPGA to operate with the EPOS2 CAN interface. The real-time operating system acts as a layer of abstraction between the broader Telescope Control System and the instrumentation hardware. For each actuator there are several variables exposed through EPICS interface that the Telescope Control System can read and write to. For example, the acquisition camera focus actuator has variables for set point position, actual position, and status, where status is a 16-bit word with each bit representing a Boolean value for enabled state, controller fault, limit switch states, set point acknowledged, target reached, and other diagnostic information. During each iteration of the real-time operating system, the current set point position is compared to the previous set point position and if the set point position is changed, a move is initiated. The actual position and status are also queried and the respective variables updated. The set point, actual position, and status information of each actuator is checked and acted upon during each iteration of the real-time operating system which takes no longer than 25ms.

## 2.2 Environment monitoring and control

In addition to the instrument control system, an independent control system is used to monitor and maintain the environment of PFIP. The Wide Field Corrector and the Focal Plane Assembly are treated as separate controlled-environment enclosures. Both subassemblies are purged with clean instrument air (FPA) or nitrogen gas (WFC). The purge gas flow rate, dew point, and temperature of both are all measured upstream of solenoid valves. The control

system monitors these sensors and actuates the solenoid valves according to a set of conditions ensuring the instrument safety. The controller, a Phoenix Contact PLC and the pre-purge sensors and solenoid valves are located in the lower electric box. A liquid leak sensor is used in the lower electric box to detect any leakage from the glycol distribution manifold also contained in the lower electric box.

Inside the Wide Field Corrector is another set of sensors monitoring the structural temperature, exterior air temperature, internal dew point, and differential pressure with respect to the exterior air. All are measured to insure a clean, dry, environment with a positive interior pressure large enough to prevent ingress of contaminants but small enough to prevent deformation or damage to the thin entrance and exit windows.

The FPA also contains two temperature sensors, a dew point sensor, and a differential pressure sensor. Additionally, there are two liquid flow meters which measure the flow rate and temperature of glycol. One flow meter measures glycol flowing through two liquid-to-air heat exchangers used to remove heat generated by the electronics. The other flow meter measures glycol flowing through the thermoelectric coolers used to cool the guide and acquisition cameras. A liquid leak sensor is also used in the FPA, with a long detection band running throughout the enclosure.

# 3. ALIGNMENT

All instrumentation in the Focal Plane Assembly (FPA) must be aligned so that it is concentric and parfocal with the Wide Field Corrector once installed on the telescope. In order to achieve alignment in the lab, a set of two common references are established. All instrumentation in the FPA is aligned to these references and the references are used to align the FPA to the Wide Field Corrector during integration on the telescope. Both references mount to through a kinematic interface with vee-blocks on the guide probe assembly. One reference, dubbed the "XYZ" reference consists of the sphere-mounted hollow retroreflector (SMR) riding on a three-axis linear stage. When aligned, the XYZ reference is located coincident with the optical axis of the Wide Field Corrector at a know distance from the focal surface. The second reference, called the "Tip Tilt" reference consists of a flat mirror on an adjustable tip-tilt stage. When aligned, the flat mirror of the Tip-Tilt reference is normal to the optical axis of the Wide Field Corrector.

Due to the construction of the guide probe assembly, the focal plane assembly references must first be aligned to the guide probe assembly. The following list outlines the order of alignment for the focal plane instrumentation:

1. Co-align "theta" bearings of guide and wave front sensor probes
2. Align FPA references
3. Align "phi" axis of guide and wave front sensor probes
4. Verify pointing of guide and wave front sensor probes
5. Align acquisition camera and fold mirror
6. Align calibration wave front sensor and fold mirror
7. Align pupil viewer camera
8. Align dithering mechanism
9. Install Focal Plane Assembly on telescope and align to Wide Field Corrector

## 3.1 Align "theta" bearings of guide probe assembly

The Guide Probe Assembly contains two guide probes and two wave front sensor probes. The four probes must be aligned to travel on a single spherical surface. Each probe has two degrees of freedom; a "theta" axis which is concentric with the optical axis of the WFC and a "phi" axis which passes through the center of the spherical focal surface at an angle of approximately 9 degrees from the theta axis. Figure 3, below illustrates the kinematics of a single probe.

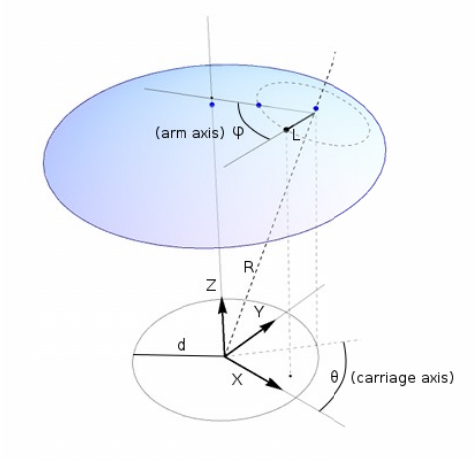


Figure 3. Illustration of the guide probe kinematics and nomenclature

The theta axis of each probe is defined by a rotary bearing and the alignment of the four bearings must be performed during assembly of the mechanism. The four bearings are installed one at a time, with each successive bearing being installed and aligned concentric with the bearings below. The first bearing installed defines the FPA central axis to which all subsequent bearings and other instrumentation will be aligned to. There is no adjustment and the bearing assembly is simply fastened to the FPA support weldment. Once the first bearing is installed, a laser tracker is setup below the assembly and a target is temporarily mounted to the moving part of the bearing. Laser tracker measurements are then recorded along the bearing's travel and a best fit circle is computed from the measurement data. The axis of the best fit circle is defined as the central axis of the entire Focal Plane Assembly. The second bearing assembly is then secured to the first bearing assembly and the laser tracker target is mounted to the moving part. Laser tracker measurements are again recorded as the second bearing is moved through a full revolution and a best fit circle is computed. The offset between the central axis and second bearing is then determined and the second bearing is moved to null the offset. The procedure is then repeated as necessary until the second bearing is concentric with the central axis and the screws holding the second bearing are fully tightened. Installation of the third and forth bearings then proceed in the same manner, aligning their measured axis with the FPA central axis.

### 3.2 Alignment of FPA references

Once the guide probe theta bearings are aligned, the FPA references can be aligned. The laser tracker is first setup below the guide probe assembly and a laser tracker target is mounted to the moving part of the bottom theta bearing. Laser tracker measurements are then recorded along the bearing's travel and a best fit circle is computed from the measurement data. The XYZ reference is then placed in the kinematic mount on the guide probe assembly and the laser tracker target is placed in the magnetic nest of the XYZ reference. The X and Y axis of the reference are then adjusted until the target is coincident with the FPA central axis.

Next, the Video Alignment Telescope (VAT) is installed in a four degree of freedom (X, Y, X', and Y') stage above the guide probe assembly. The laser tracker target is placed on the barrel of the VAT and swept over the barrel's surface while laser tracker measurements are recorded. A best fit cylinder is then computed from the measurements and the angular offset between the VAT barrel and the FPA central axis is found. Tip and tilt adjustments are then made to the VAT stage and procedure is repeated as needed until then axis of the VAT is parallel with the FPA central axis. The Tip-Tilt reference is then placed in the kinematic mount on the guide probe assembly. The VAT is then used in autocollimator mode to find the angular offset between FPA central axis and flat mirror on the Tip-Tilt reference. Micrometer adjusters on the Tip-Tilt reference are then used to null the offset until the flat mirror is normal to the FPA central axis. The Tip-Tilt reference adjusters are then locked and their settings recorded.

### 3.3 Alignment of phi axis of guide and wave front sensor probes

The "phi" axis of each probe is adjustable in tip, tilt, and piston. The purpose of the adjustments are to align the phi axis such that it intersects the FPA central axis and does so at an axial location such that the probe optical head moves on a spherical surface which is concentric with the spherical focal surface produced by the Wide Field Corrector. A special probe head was fabricated which holds a laser tracker target at a precisely known location with respect to the phi axis of

a guide probe or wave front sensor assembly. Figure 4, below shows the laser tracker target probe and a wave front sensor probe head. The probe was then driven through a raster pattern through its full range of motion with laser tracker measurements taken for each millimeter of linear travel. The laser tracker measurements are then compared to an ideal spherical surface with radius and center point constrained in the ideal optical location with respect to the FPA references. The error vectors from measured points to ideal spherical surface are then analyzed to determine the required adjustments of the phi axis orientation. Error vector magnitudes that monotonically increase or decrease as a function of phi axis position requires adjustment to the "tip" of the probe, effectively changing the radius of curvature of the actual spherical surface swept by the probe. Error vector magnitudes which are parabolic as a function of phi axis position require adjustment to the "tilt" of the probe so that the phi axis intersects the theta axis. Each probe is iteratively measured and adjusted until the error magnitudes are below 35 microns.

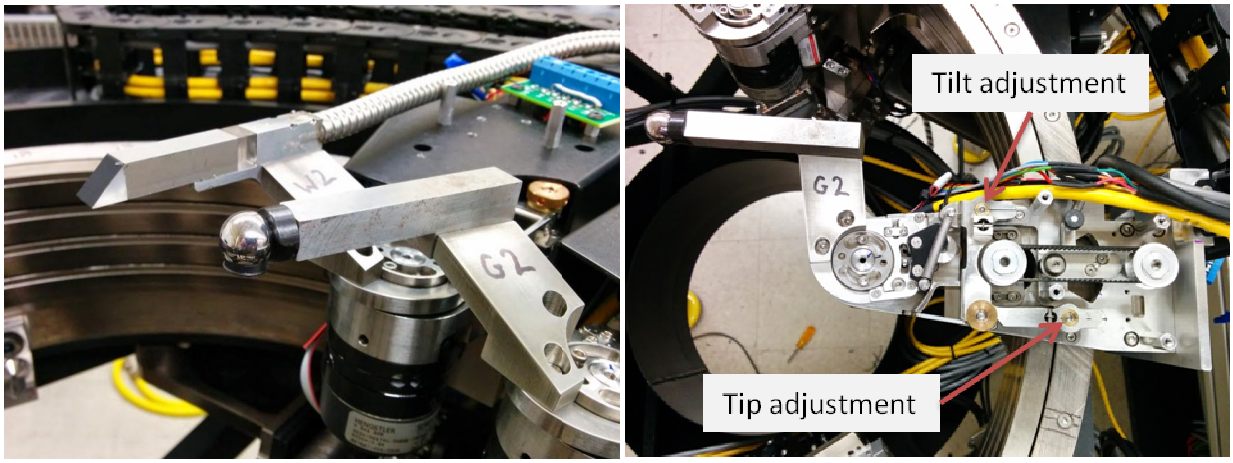


Figure 4, left, shows a wave front sensor probe and a laser tracker target probe for alignment. Figure 5, right, shows the tip and tilt adjustment screws for the guide probes.

### 3.4 Verify pointing of guide and wave front sensor probes

While the guide and wave front sensor probes are adjustable in the kinematics of their motion, no independent adjustment of the probes pointing is available. It is assumed that the fabrication tolerances of the probes are sufficiently tight that even in the worst case phi axis adjustment, the probe pointing is acceptable. A test was devised to verify this by using the wave front sensor probe heads to image a target placed at the pupil position. A LCD computer monitor was used as the target, with a crosshair image displayed at the same size as the pupil created by the Wide Field Corrector. The Video Alignment Telescope was first setup above the guide probe assembly and aligned to the FPA references. The LCD monitor was secured to a six degree of freedom stage and adjusted so that the crosshair displayed by the target was aligned to the VAT crosshair. The VAT was then used in autocollimator mode to adjust the LCD target so that it was normal to VAT axis. The laser tracker was then used to measure and adjust the axial distance between the FPA reference and LCD target to match the telescope's optical design.

With the LCD target in place at the pupil, the projected image was changed from a crosshair to an annulus with the same size as the illuminated portion of the Wide Field Corrector pupil. A wave front sensor probe head was mounted to a probe and images were recorded as the probe was moved through it range of travel. The pupil target was verified to be sufficiently centered on the wave front sensor image and that the target center was stationary on the image throughout the travel of the probe. A sample image is shown in figure 6, below. The wave front sensor probe head was then removed and replaced on the other three probes, verifying the pointing of each. Figure 7 shows the LCD pupil target setup below the guide probe assembly.

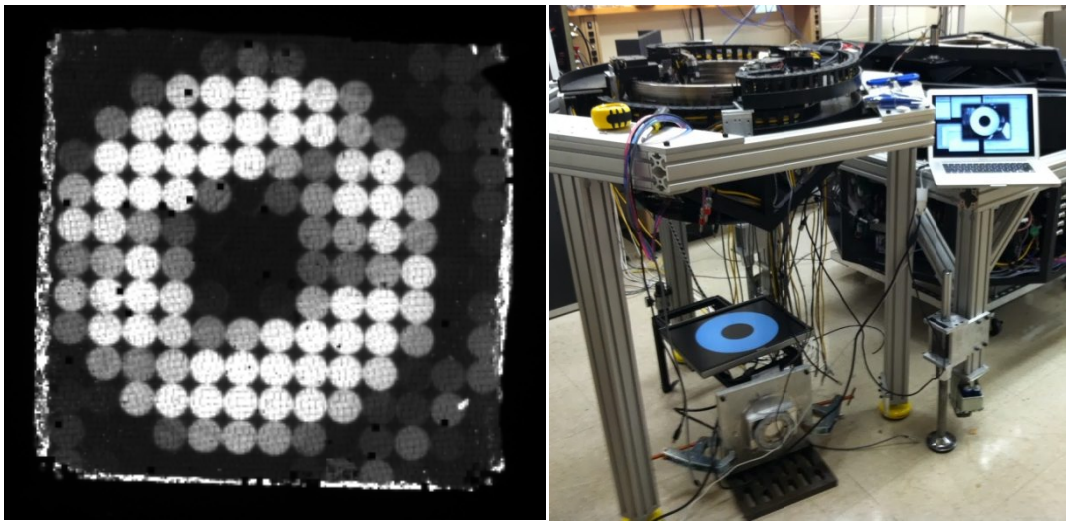

Figure 6, left, shows a sample image from the wave front sensor probe viewing the LCD pupil target. Figure 7, right, shows the LCD pupil target setup below the guide probe assembly.

### 3.5 Align acquisition camera and fold mirror

The acquisition camera and the deployable fold mirror which feeds light to the camera are aligned by using the Video Alignment Telescope to project an image onto camera. The VAT is placed on a six degree of freedom stage below the acquisition and guiding assembly and aligned in X, Y, tip, and tilt to the FPA references. The FPA references are then removed and the fold mirror deployed. The acquisition camera shutter is then removed and the VAT focus adjusted to image the camera's CCD. The VAT reticle is illuminated and an image from the acquisition camera is recorded. An example of the acquisition camera image with the VAT reticle projected onto the CCD is shown in figure 8, below. The location of the reticle center within the acquisition camera image is then compared to the position predicted by ray-tracing in Solidworks and the fold mirror is adjusted in tip and tilt to null the error. Next, the VAT is put into autocollimator mode and a flat mirror is placed on the mounting flange of the acquisition camera. The VAT is then used to verify that the mounting flange, and by extension the CCD, is normal to the optical axis. While adequate alignment was achieved through fabrication tolerances of the assembly, adjustments are possible by shimming the kinematic vee blocks used to mount the acquisition camera assembly. A photo of the setup is shown in figure 9, below.

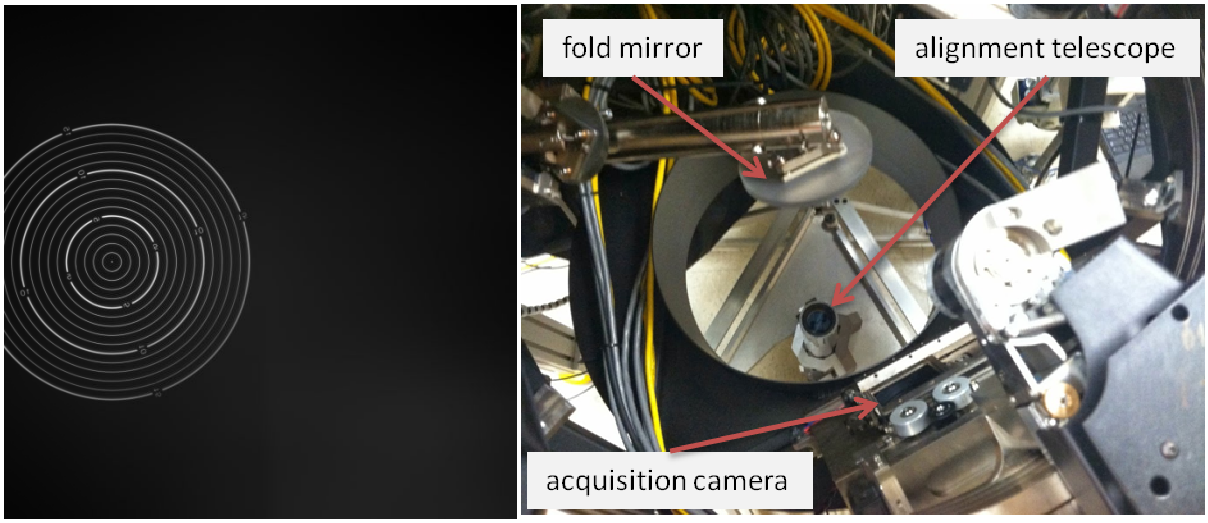


Figure 8, left, shows a sample image of VAT reticle projected onto the acquisition camera. Figure 9, right, shows the hardware setup for acquisition camera alignment.

### 3.6 Align calibration wave front sensor and fold mirror

The fold mirror which feeds the calibration wave front sensor is first aligned by viewing the field stop of the calibration wave front sensor through the VAT. The VAT is placed on a six degree of freedom stage below the acquisition and guiding assembly and aligned in X, Y, tip, and tilt to the FPA references. The FPA references are then removed and the fold mirror deployed. The VAT focus is then adjusted so that the field stop of the calibration wave front sensor is visible. The fold mirror is then adjusted in tip and tilt so that the circular field stop is centered on the reticle crosshair of the VAT. Next, the tip and tilt of the calibration wave front sensor is aligned by turning on the illuminated reticle of the VAT and viewing the image recorded by the calibration wave front sensor. The tip and tilt of the sensor is set using three screws on the front of the assembly and adjusted so that the center dot of the VAT reticle projection is centered on the central lenslet of the wave front sensor image. The tip and tilt adjustment screw locations are shown in figure 10. An example image of the misaligned sensor is shown in figure 11 and an example of the aligned sensor is shown in figure 12.

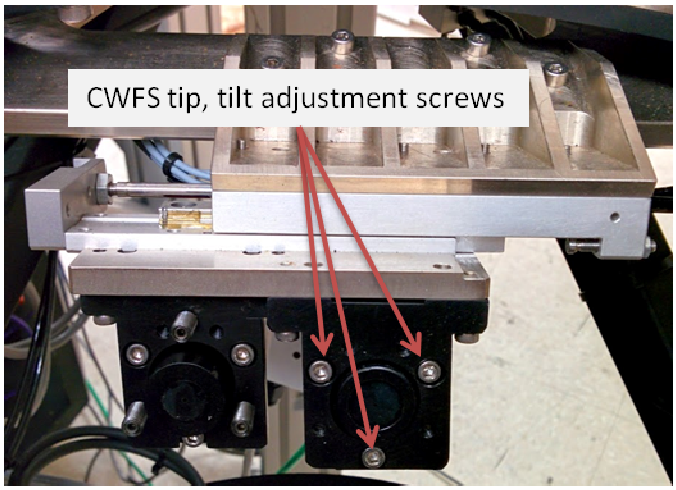


Figure 10 indicating the location of the tip and tilt adjustment screws for the calibration wave front sensor.

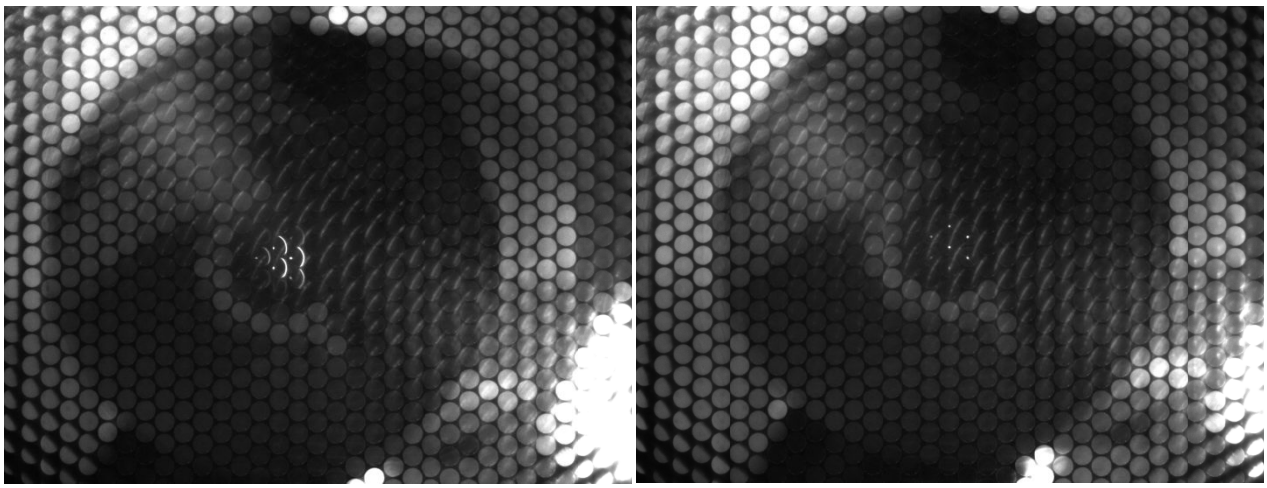

Figure 11, left, shows an example image from the misaligned calibration wave front sensor when the VAT is used to project a reticle onto the camera. Figure 12, right, shows an example image from the aligned calibration wave front sensor.

Once the calibration wave front sensor is aligned in tip and tilt, it is verified by imaging a target at the pupil. The VAT is first removed from under the acquisition and guiding assembly and replaced by the LCD pupil target on its six degree of freedom stage. The VAT is then setup above the acquisition and guiding assembly and aligned in the same fashion described in section 3.4. An image was then displayed on the LCD pupil target showing an annulus with the same size as the illuminated portion of the Wide Field Corrector including obstructions from the tracker assembly. The calibration

wave front sensor image was recorded and the image analyzed to verify that it is adequately centered. Figure 13, below shows and example image recorded by the calibration wave front sensor.

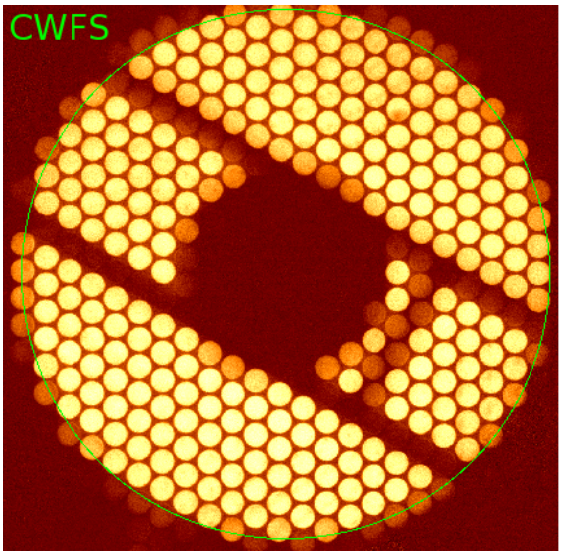


Figure 13. An image from the calibration wave front sensor viewing the LCD pupil target for verification of alignment

### 3.7 Align pupil viewer

The pupil viewer is fed by the same fold mirror as the calibration wave front sensor and therefore the fold mirror is not adjusted during alignment of the pupil viewer. Only the tip and tilt is adjusted, as well as the travel of the linear stage which deploys either pupil viewer or calibration wave front sensor into the optical path of the fold mirror. The adjustment screws are noted in figure 14. The VAT is first set up below the acquisition and guiding assembly in the same manner as outlined in section 3.6. The fold mirror is deployed and the pupil viewer is deployed into position so that the VAT can view the field stop of the pupil viewer. The travel adjustment screw is then set so that the pupil viewer field stop is centered on the VAT crosshair reticle. The VAT is then removed and the LCD pupil target is placed under the acquisition and guiding assembly in the same manner as described in section 3.4. The pupil viewer images are then recorded and the tip and tilt adjustment screws set so that the image of the pupil is completely visible on the fold mirror, as shown in figure 15.

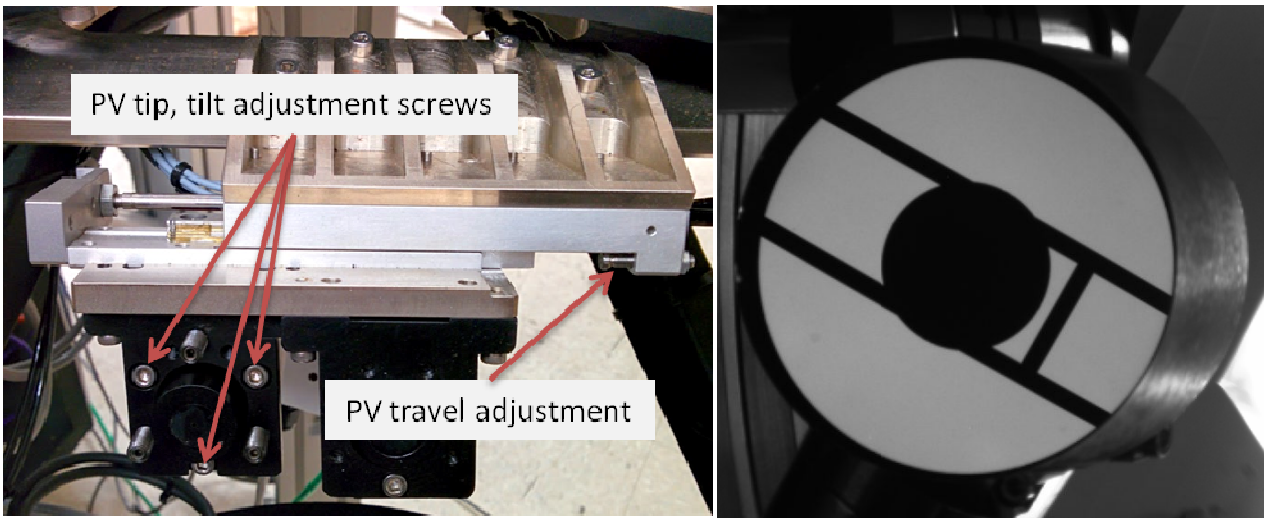


Figure 14, left, shows the tip and tilt adjustment screws for the pupil viewer camera. Figure 15, right, shows an example image from the pupil viewer with an image of the LCD pupil target contained on the fold mirror.

### 3.8 Align dithering mechanism

The dithering mechanism holds the input head mount plate (IHMP) and all the science fiber feeds above the main shutter. This subassembly must be aligned parfocal and concentric with the acquisition and guiding assembly which is situated below the main shutter. To start alignment, the acquisition and guiding assembly must be removed from its laboratory stand and mounted to the focal plane assembly weldment. The VAT is then placed under the acquisition and guiding assembly and aligned to the FPA references as described in section 3.2. The IHMP is then fitted with the alignment center plug, shown in figure 16, and a flat mirror placed on the top surface of the center plug. With the VAT set in autocollimator mode, the tip and tilt of the dithering mechanism is adjusted with shims so that the flat mirror on the IHMP center plug is parallel with the FPA tip tilt reference. Shims are to be placed under the vee blocks on the shutter plate. Next, the FPA XYZ reference is placed in the guide probe assembly and the laser tracker is setup above the dithering mechanism so that it has a line of sight through the IHMP center plug to the FPA XYZ reference. The laser tracker is then used to measure the distance between the FPA XYZ reference and the IHMP center plug. Shims are then selected to adjust the distance so that the center of the spherical surface found during alignment of the guide probes is 995.6mm from the laser tracker target on the IHMP center plug.

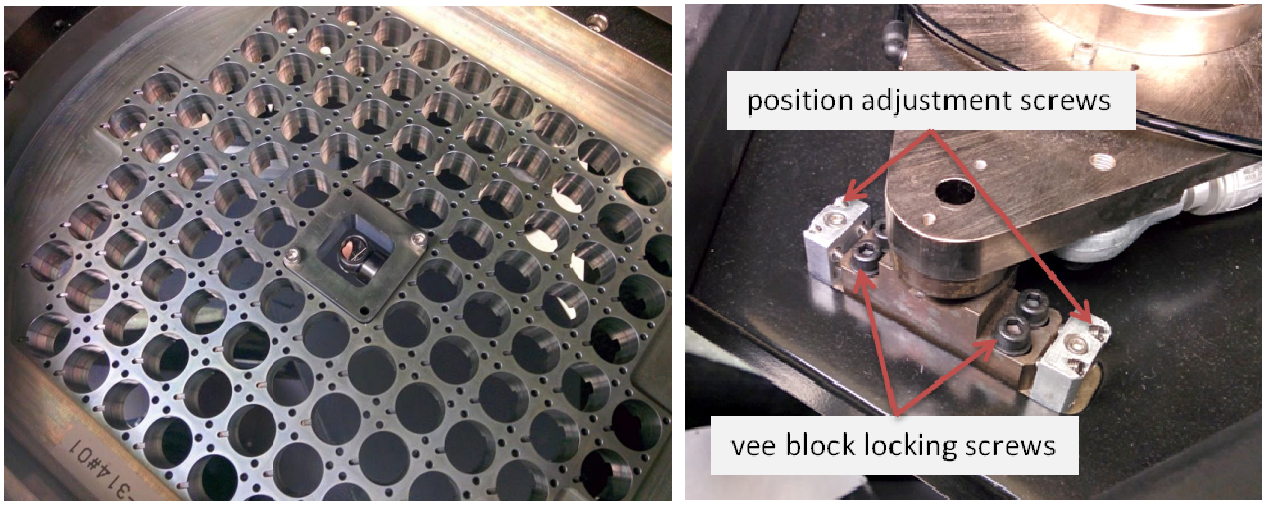


Figure 16, left, shows the alignment center plug installed in the IHMP with a laser tracker target. Figure 17, right, shows the lateral adjustment for the dithering mechanism.

After the dithering mechanism is aligned in tip, tilt, and piston, the VAT is used to align in centration. The laser tracker target on the IHMP center plug is turned so that it is facing the VAT and the VAT images are recorded to view the position of the target with respect to the VAT crosshair reticle. The X and Y position of the dithering mechanism is then adjusted by moving the vee blocks on the shutter plate as shown in figure 17.

### 3.9 Install Focal Plane Assembly and align with Wide Field Corrector

Once all instrumentation in the FPA is co-aligned, it can be installed onto the telescope and aligned with the wide field corrector. Alignment requires both VAT and laser tracker, with the VAT being installed on its six degree of freedom stage at the bottom of the Wide Field Corrector. The laser tracker is installed on the pupil plane assembly, as shown in figure 18. The VAT is first aligned to references on the M4 optic in the Wide Field Corrector in X, Y, tip, and tilt. The FPA references are then viewed with the VAT and adjustments are made to the PFIP support structure legs, first aligning in X and Y using the crosshair reticle and then changing to autocollimator mode and aligning tip and tilt.

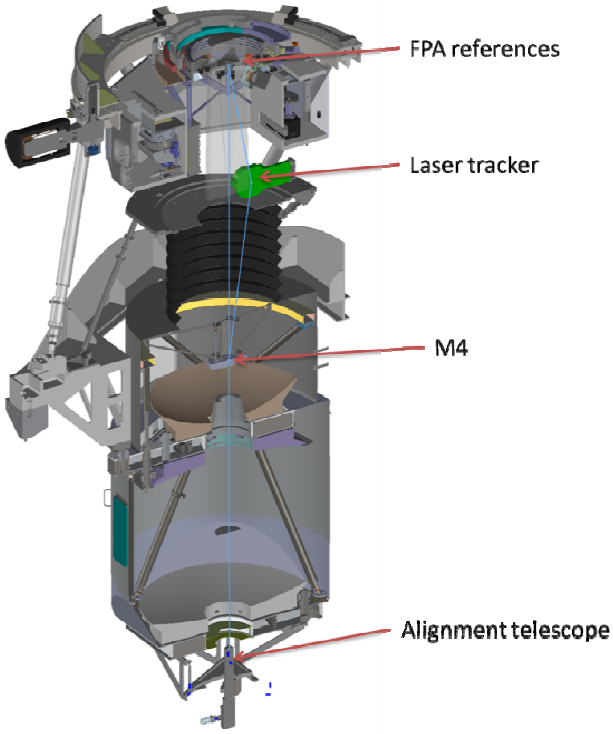


Figure 18 showing the lines of sight for the laser tracker and VAT during alignment of the FPA to the Wide Field Corrector

## 4. COLD TESTING

In order to verify the operation of the PFIP instrumentation during cold weather, a campaign of low temperature testing was performed. Since there is no convenient environmental testing facility available at the University of Texas, a refrigerated truck was rented from a local Ryder brand rental company. The truck had an 8 meter long insulated cargo bay with roll-up door and hydraulic lift for easy loading. An auxiliary diesel engine powered the refrigeration unit which easily and quickly cooled the cargo bay to -10C, the lower operating requirement for the HET. All instrumentation and electronics was loaded into the cargo bay with only 110VAC and Ethernet passing through to a control computer and power source outside of the truck. The control computer was programmed with a routine to exercise all axis of motion, record images from all cameras, and monitor the environmental sensors. Figure 19 shows the instrumentation and electronics loaded in the refrigerated truck.

Several problems surfaced during the cold testing. The first problem was due to an encoder cable which lost much of its flexibility under the cold conditions. The encoder cable ran through a cable carrier on the guide probes and the motion caused the encoder cable to pull free from its connector. This resulted in an intermittent fault which proved difficult to find since warming the cargo bay to a temperature suitable for extended troubleshooting eliminated the problem. The issue was resolved by anchoring the cables at both ends of the cable carrier.

The second problem found under cold temperatures presented as following errors occurring on two of the guide probes, on the “theta” axis of motion. Monitoring the motor current showed that the motors were drawing the maximum current, set in the servo controller to maintain safe motor winding temperature during continuous operation. Moving the guide probes by hand confirmed that the force required to move the two guide probes experiencing problems was much greater than the two guide probes not experiencing problems. Two separate issues are believed to have contributed to the low temperature failures. The two guide probes experiencing problems had components which were manufactured out of specification. These were the parts that mate to the large rotary bearings. While their manufacturing defects were known, the effect on optical performance was negligible. The effect on motion performance was not appreciated until cold testing. The offending components were subsequently replaced. The other issue was due to the lubrication used in the rotary bearings. Since common grease is prohibited in the FPA instrumentation, the rotary bearings were lubricated with a thin film of high vacuum grease, which was thought to be more stable over long periods of time. However, the

high vacuum grease became highly viscous at low temperatures and contributed to the resistance of motion of the bearings. The bearings were cleaned and a dry film lubricant was used. Testing the longevity of this lubricant is ongoing, but the initial results show no degradation over an approximate year's worth of simulated usage.

Figure 19. The FPA instrumentation and electronics setup in the refrigerated truck for cold testing

## 5. 3D PRINTING

The proliferation of inexpensive 3D printers in the last few years has opened significant design space in mechanical engineering and PFIP takes advantage of this in several ways. The project purchased a Makerbot Replicator 2, which is a consumer-grade 3D printer capable of producing objects made of polylactic acid based plastics (PLA) up to 285 x 153 x 155mm in size. The limitations of 3D plastic printing process and the advantages over traditional fabrication techniques tend to drive the design and application of such parts. The dimensional accuracy of objects printed with the Replicator are on the order of 0.2mm in practice. This would generally preclude its use producing parts for typical astronomy instrumentation. Additionally, little data exists on the long-term stability and outgassing properties of PLA plastics. For these reasons, 3D printed parts are only being used in non-structural, non-critical, or temporary applications. Conversely, the ability of 3D printers to produce thin-walled and geometrically complex parts provide a capability not practically possible in subtractive machining. For example, the guide probe mechanisms include motors and encoders which are located in close proximity to light near the telescope's focus. A cover was needed to baffle these components and prevent them from reflecting stray light. The space constraints and complex shape required would have made traditional fabrication processes impractical. Using our 3D printer, a thin-walled plastic housing was fabricated for less than $1USD in material costs. The cover has wall thickness varying from 0.4mm to 5mm and contains an internal hex cell structure to increase rigidity. Figure 20 shows two guide probe assemblies; one with and one without the plastic housing.

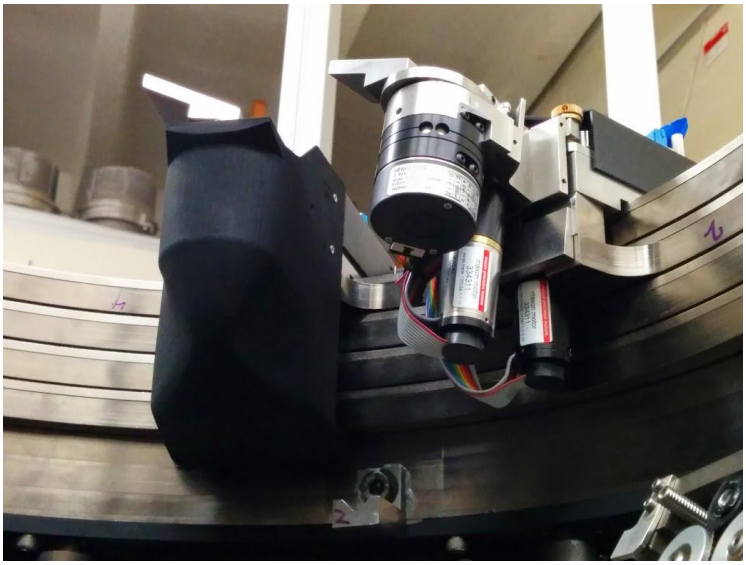

Figure 20. Guide probes with and without 3D printed plastic housing

Another benefit of 3D printers is the relatively quick turnaround for making parts. This is particularly useful in the laboratory during alignment and calibration tasks. Oftentimes the process of alignment reveals an unexpected need for a part and as a result the process must be delayed for days for a commercial parts to be ordered and delivered or weeks for a custom part to be fabricated. Parts produced from a 3D printer can usually be made in a few hours or overnight and since the printing process is automated, no personnel resource need be expended.

## ACKNOWLEDGEMENTS

HETDEX is run by the University of Texas at Austin McDonald Observatory and Department of Astronomy with participation from the Ludwig-Maximilians-Universität München, Max-Planck-Institut für Extraterrestriche-Physik (MPE), Leibniz-Institut für Astrophysik Potsdam (AIP), Texas A&M University, Pennsylvania State University, Institut für Astrophysik Göttingen (IAG), University of Oxford and Max-Planck-Institut für Astrophysik (MPA). In addition to Institutional support, HETDEX is funded by the National Science Foundation (grant AST-0926815), the State of Texas, the US Air Force (AFRL FA9451-04-2-0355), by the Texas Norman Hackerman Advanced Research Program under grants 003658-0005-2006 and 003658-0295-2007, and by generous support from private individuals and foundations.

## REFERENCES

[1] Hill, G.J., Drory, N., Good, J., Lee, H., Vattiat, B.L., Kriel, H., Bryant, R., Elliot, L., Landiau, M., Leck, R., Perry, D., Ramsey, J., Savage, R., Damm, G., Fowler, J., Gebhardt, K., MacQueen, P.J., Martin, J., Ramsey, L.W., Shetrone, M., Schroeder, E., Cornell, M.E., Booth, J.A., Walter Moriera, W., "Deployment of the Hobby-Eberly Telescope Wide Field Upgrade", Proc. SPIE, **9145**-5 (2014)

[2] J.H. Beno, C.E. Penney, R.J. Hayes, I.M. Soukup, "HETDEX tracker control system design and implementation," Proc. SPIE, **8444**-211 (2012)

[3] J.J. Zierer, Jr., G.A. Wedeking, J.H. Beno, J.M. Good, "Design, testing, and installation of a high-precision hexapod for the Hobby-Eberly Telescope dark energy experiment (HETDEX)," Proc. SPIE, **8444**-176 (2012)

[4] H. Lee, G.J. Hill, M.E. Cornell, B.L. Vattiat, T.H. Rafferty, C.A. Taylor III, D.M. Perry, C. Ramiller, M. Hart, M.D. Rafal, R.D. Savage, "Metrology systems of Hobby-Eberly Telescope wide field upgrade," Proc. SPIE, **8444**-181 (2012)

[5] B.L. Vattiat, et al., "Design, testing, and performance of the Hobby Eberly Telescope prime focus instrument package," Proc. SPIE, 8446-269 (2012)